MATHEMATICA MONTISNIGRI
Vol LVII (2023)

EQUATIONS OF STATE OF THE MOLTEN AND CRYSTALLINE PHASES OF ALUMINUM WITH DEEP ENTRY INTO METASTABLE REGIONS

V.I. MAZHUKIN, M.M. DEMIN, A.V. SHAPRANOV, O.N. KOROLEVA*, A.V. MAZHUKIN

Keldysh Institute of Applied Mathematics RAS, Moscow, Russia
* Corresponding author. E-mail: koroleva.on@mail.ru

DOI: 10.20948/mathmontis-2023-57-6

Summary. The article is devoted to the problem of constructing equations of state with deep entry into metastable regions (overheating/undercooling) of the molten and crystalline phases of aluminum. For mathematical modeling of hydrodynamic processes, the knowledge of the equations of state is the source of the most important information about the dependence of the thermodynamic properties of a substance on the microscopic internal structure. Moreover, for modeling, the equations of state are required in the form of smooth analytical dependencies with the characteristics of metastable states. Molecular dynamics simulation was used as the main tool for obtaining the equations of state. Based on the results of molecular dynamics calculations, the work obtained mutually consistent single-phase equations of state for molten and crystalline aluminum in tabular form. For tabular values, the approximating analytical dependences of low degrees were obtained. The results are presented in the form of tables and graphs. The thermodynamic consistency of the resulting equations is investigated. The simulation results of this work are compared with the equations of state for aluminum obtained by other authors.

1 INTRODUCTION

One of the most difficult problems facing mathematical modeling of hydrodynamic processes is the correct estimation and choosing of the equation of state (EOS). The knowledge of the EOS of a substance is important for its information content about the dependence of the thermodynamic properties of a substance on the microscopic internal structure, which makes EOS an inevitable component of all hydrodynamic models. Currently, there is no unified approach to creating a high-precision theory for determining the thermodynamic properties of matter in a fairly wide region of phase space, since the knowledge about these states in such a wide range is always limited. The necessary information can be obtained in two ways: using theoretical modeling [1-5] or using complex experiments [6-8]. However, obtaining a high-precision distribution of thermodynamic parameters using mathematical modeling is limited by the range of applicability of the models used, and the experimental studies are hampered by the complexity of their implementation.

In recent years, more and more attention has been paid to the states of matter with high and ultra-high energy densities, which are responsible for achieving high pressures and temperatures. Contemporary interest in extreme states of matter is driven by the rapid growth of scientific and technological applications related to the physics of extreme states. Extreme

2020 Mathematics Subject Classification: 82M37, 70-10, 76-10, 80-10.
Key words and Phrases: Equations of state, molecular dynamics modeling, metastable regions, hydrodynamic processes, thermodynamic matching

states arise when a substance is exposed to intense shock [9], detonation [10], electroexplosive waves [11], intense electron-ion beams [12], concentrated streams of laser radiation [13, 14], etc.

An unsteady hydrodynamic process is characterized by a change in four macroscopic variables: velocity, density, pressure and internal energy of the material. These four parameters are described by the hydrodynamic equations based on the laws of conservation of mass, momentum and energy, as well as by the equation of state (EOS), which formally relates pressure, density and energy.

The construction of the EOS, consisting of experimental measurements and theoretical calculations of pressure-volume-temperature (P, V, T), plays a huge role, which stimulates intensive research into the properties of materials in both fundamental and applied fields of science. Thus, fundamental studies of plasma physics using intense beams of heavy ions and lasers [15,16] have shown that ion beams and laser beams make it possible to concentrate energy in space and time in such a way that matter can be converted into plasma with a solid-state density. As a result, the atomic and ionic states turn out to be mixed and very different from the original atomic states. Their characteristics can be expressed through the EOS, which relates pressure and temperature to the density of the sample, via the properties of electrical conductivity, thermal conductivity and radiative transfer. In basic sciences, EOS are often used to test the quality of theoretical models [17]. EOS play a major role in studies of the dynamics of phase transitions: solid - liquid [18], liquid - vapor [19], plasma - dielectric [20], etc.

In applied sciences, the importance of EOS is determined by the need to use their initial data in hydrodynamic calculations in such problems as the development of processing technologies [21, 22], modification of structural and functional materials by ultrashort high-power laser pulses [23]

High energy density physics deals with the EOS of matter over a very wide range of phase diagrams: from a compressed solid (crystal) to dense hot liquid, vaporized and ionized matter (non-ideal plasma), characterized by extremely high pressure and temperature. As already noted, the EOS of a substance is an external equation with respect to the conservation laws and is constructed either from the results of experiments [24] or by methods of statistical physics [25]. At the same time, taking into account the size of the phase space region, a difficult choice arises: to use only one wide-range EOS equation over the entire range or to switch between different equations, depending on changes in thermophysical parameters. For numerical modeling of processes in substances with high or ultra-high energy density, it is preferable to use wide-range EOS equations [26, 27], the development of which faces a number of difficulties. The main difficulty in the consistent theoretical calculation of the EOS of a substance using statistical physics methods is the need to correctly take into account the complex structure of interparticle interactions in the quantum mechanical many-body problem for any values of the coupling constant and any type of statistics [5]. Due to the limited scope of application of each of the methods used, none of them can provide a complete theoretical representation of the thermodynamic properties of a substance over the entire phase plane from a cold crystal to liquid and hot plasma [18, 28]. Therefore, when constructing wide-range EOS, it is necessary to use simplified models, the scope of which is limited and is established individually in each specific case, either using the internal characteristics of the model, or through comparison with exact solutions, if they exist, or comparison with experimental results. The most widely used data are experimental measurements, which are

used to choose the numerical parameters in the functional dependencies constructed on the basis of exact solutions or simplified models. The semi-empirical models obtained in this way are used to describe and formulate adequate zero-approximation models in particularly complex situations (liquids, solids, dense plasma). The success of constructing semi-empirical EOS models is verified both by the quality of the heterogeneous experimental data used and by the possibility of using extrapolation calculations.

The information obtained in dynamic experiments [29] significantly expands the basic understanding of the physical properties of matter in a wide region of the phase diagram up to ultra-high pressures and temperatures. Currently, shock wave methods provide the most important practical information for creating a wide range of EOS [30]. The most powerful EOS are based on sound theoretical models and describe a wide range of phase diagrams with high accuracy and reliability. Its high accuracy allows EOS to be used in advanced numerical simulations to solve numerous high-energy-density physics problems.

One of the significant drawbacks of semi-empirical EOS is the lack of an adequate description of the region of metastable states in phase transformations, despite the correct description of the melting/crystallization and evaporation/condensation phase boundaries [26].

However, strongly overheated or undercooled metastable states can have a significant impact on the dynamics and nature of phase transformations. In oder to simulate these features one neeeds an EOS containing a description of these metastable states.

The purpose of this work is to construct mutually consistent single-phase equations of state (thermal, caloric) with deep penetration into the metastable regions (overheating/undercooling) of the molten and crystalline phases of aluminum.

2 STATEMENT OF THE PROBLEM

In the problem of mathematical modeling of metal ablation by ultrashort high-power laser pulses using continuum hydrodynamic models, the choice of the equation of state plays an important role. The difficulties associated with the choice and construction of EOS are determined by the specifics of the action of femtosecond laser radiation on solid targets [31,32]. The hydrodynamic models used are developed on the basis of fundamental knowledge of the physics of nonequilibrium processes, which allows them to most fully cover the basic mechanisms of ablation. The main feature of femtosecond action on metals in the temperature range $T_0 \le T < T_{cr}$ (where T_0, T_{cr} are the room and critical temperature correspondingly), consists in the occurrence of rapid phase transitions accompanied by metastable highly overheated/undercooled states.

As noted above, the construction of EOS is based on the widespread use of both complex theoretical models [4,5,33] and extensive experimental data [34,35]. However, the construction of EOS for metals exposed to ultra-short ultra-high-power laser radiation faces great difficulties. As a result, none of the available approaches could be applied to the construction of EOS. The main reason is that, due to the extremely short time frame in which nonequilibrium processes develop, the behavior of metals is extremely difficult to study experimentally. Information about the mechanisms of the main processes is obtained mainly from theoretical calculations and predictions.

In this situation, the most effective method for constructing EOS turned out to be molecular dynamics modeling, which allows one to sufficiently fully and accurately characterize the parameters of the metastable region.

Usually two types of equations of state are considered: thermal - $P(\rho,T)$ and caloric - $E(\rho,T)$. In one of them, pressure P, and in the other, respectively, internal energy E, are the functions of temperature T and density ρ. These EOS are presented in the form of tables, or in the form of analytical dependencies. The authors of this work required an EOS that would be applicable to the numerical solution of the previously developed continuum hydrodynamic model of laser heating and fragmentation of an aluminum target [36,37]. The algorithm for the numerical solution of this model is based on the dynamic adaptation method [38, 39], which makes it possible to perform calculations with the explicit tracking of an arbitrary number of phase boundaries [40, 41], contact boundaries [42], and shock wave fronts [43, 44]. In this case, at each of the phase boundaries, the boundary conditions are used in which pressure is calculated both through density and temperature, and vice versa, density is calculated through pressure and temperature. This requirement is met by EOS without areas of ambiguous correspondence between ρ and P. In other words, it is necessary that for all isotherms of each phase the condition that the pressure derivative with respect to density is not equal to zero $(\partial P/\partial\rho \neq 0)$.

Taking into account the fact that the original hydrodynamic model is approximated by a family of implicit difference schemes, the numerical implementation of which is carried out by iterative methods, and the numerical solution of nonlinear boundary conditions in the finite-difference approximation is carried out by specially constructed iterative procedures, additional requirements are imposed on the developed EOS. It is desirable to ensure the best convergence of all iterative processes used and, thereby, to ensure the possibility of calculations with large time steps. To do this, it is necessary to have a smooth analytical thermal EOS, which would explicitly express pressure in terms of density and density in terms of pressure. As specially carried out calculations have shown, it is the smoothness of the thermal equation of state that has the greatest effect on the convergence of iterative procedures.

3 MATHEMATICAL MODEL

The molecular dynamics (MD) method is based on a model representation of a system of N point atoms, the motion of which is described in the classical case by Newton's equations. Thus, there is a system of $2N$ equations:

$$\begin{cases} m_i \dfrac{d\vec{\upsilon}_i}{dt} = \vec{F}_i + \vec{F}_i^{ext} \\ \dfrac{d\vec{r}_i}{dt} = \vec{\upsilon}_i \end{cases} \qquad i = 1 \ldots N \tag{1}$$

where m_i, υ_i, r_i are mass, velocity and radius-vector of i-th atom, F_i, F_i^{ext} are the force of interation with other atoms and that with the external field for the i-th atom. The semi-empirical potential of the "embedded atom method" (EAM), presented in [45], was used as the potential.

The Maxwell distribution at double the initial temperature is used as the initial conditions for the velocities. For the initial distribution of atomic coordinates, an ideal fcc lattice with a

given lattice parameter is taken. Periodic boundary conditions are specified at the boundaries of the region.

To numerically solve this system of equations, we used the Verlet scheme [46], implemented within the open LAMMPS package [47].

4 COMPUTATIONAL EXPERIMENT

4.1 Thermal equation of state $P(\rho,T)$

The configuration of the atoms is chosen in the form of a cube with a size of 18×18×18 elementary cells or 7.26×7.26×7.26 nm^3 with the value of the lattice parameter for a given EAM potential of 0.4032 nm. A FCC lattice of 23328 aluminum atoms is placed in this area. Periodic boundary conditions are set along all three axes. The integration step is set to 1 fs.

Initially, the atoms are located in the nodes of the FCC lattice, and the particle velocities are set according to the Maxwell distribution. The sample is equilibrated at a temperature of 300 K and zero pressure using a thermostat and a Berendsen barostat. This state was used as the initial one for the subsequent series of measurement experiments to obtain the equation of state of the solid phase.

Each experiment was performed as follows. The sample was compressed uniformly in three main crystallographic directions ((1,0,0), (0,1,0), (0,0,1)) up to a pressure of about 100 GPa. At the same time, the required temperature value was set by the thermostat. Further, keeping the temperature constant, the pressure was lowered to the required values, and at each such value the sample relaxed for 100 ps. After relaxation, the average density value was obtained. The pressure values were lowered until melting or rupture of the sample occurred. Thus, a single-phase isotherm for the crystal was obtained.

To obtain the equation of state of the liquid, the initial state was chosen by heating to a temperature above the melting point. At the same time, the sample was melting. After that, it was cooled by a thermostat to the melting point.

Then, to determine the thermal equation of state, the sample at a fixed temperature was compressed by a barostat to the required pressure and held for 100 ps. In this state, the resulting average density was obtained. The pressure was set from -7 to 9 GPa with a step of 1 GPa and then from 10 to 90 GPa with a step of 20 GPa. Several temperature values were chosen for which these dependencies were obtained: for a solid 300, 600, 900 and 1500 K, and for a liquid 950, 2000, 3500, 5000 and 6500 K. The results of these measurements are given in table. 1(a) and 2(a) of the appendix.

Then the following function was constructed approximating these results:

$$\begin{aligned} P(\rho,T) &= a(T)\rho^2 + b(T)\rho + c(T) \\ a(T) &= \alpha_a T^2 + \beta_a T + \gamma_a \\ b(T) &= \alpha_b T^2 + \beta_b T + \gamma_b \\ c(T) &= \alpha_c T^2 + \beta_c T + \gamma_c \end{aligned} \qquad (2)$$

Here the dimensions of density are g/cm^3, pressure - GPa, temperature - K. The coefficients α, β, γ for the solid and liquid phases are given in Table. 1(b) and 2(b) of the appendix. The range of applicability of the obtained approximating functions is assumed to correspond to the extreme values of tables 1(a), 2(a).

Figs. 1, 2 show the obtained isotherms for the solid and liquid phases: (a) – the results of MD modeling (circles) and their approximation by the analytical function (solid lines). (b) – an enlarged fragment, black dash-dotted and solid lines – lines of equilibrium melting and maximum overheating/undercooling, respectively. Yellow markers indicate the metastable areas located between these lines.

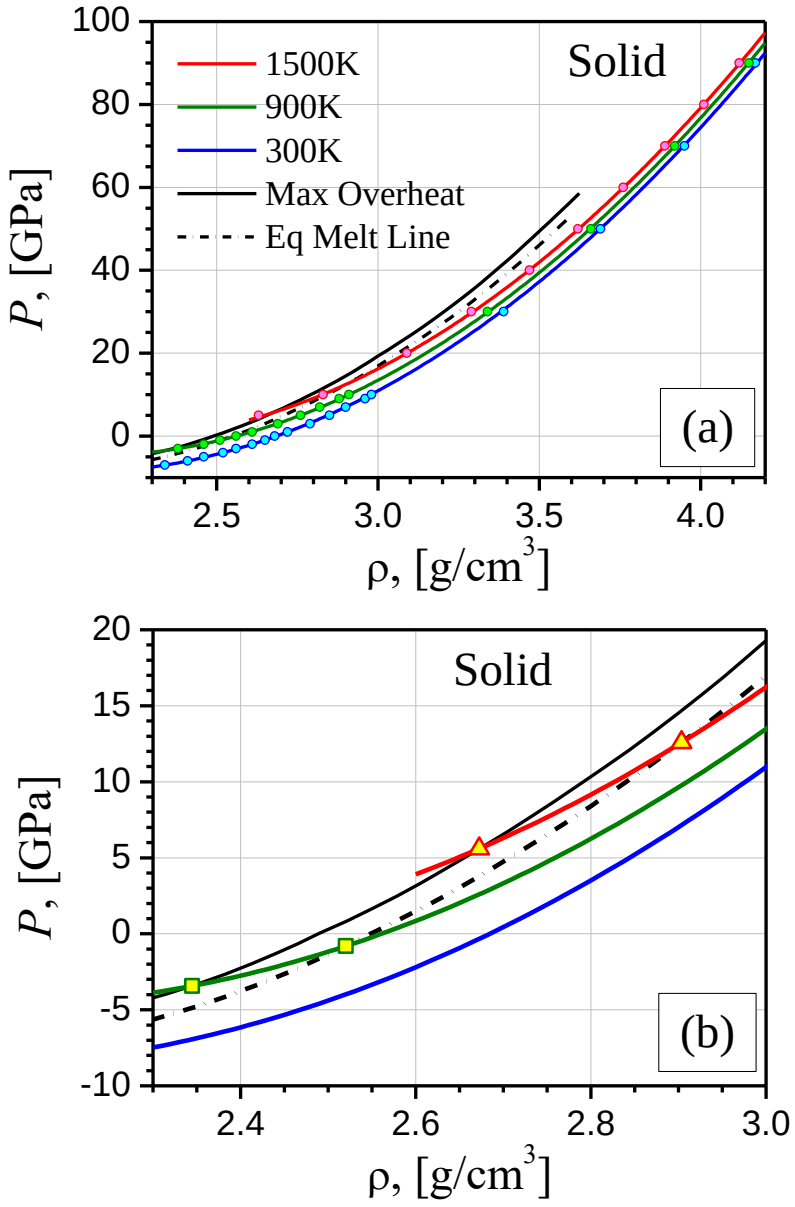

Fig.1. Isotherms for the solid phase.

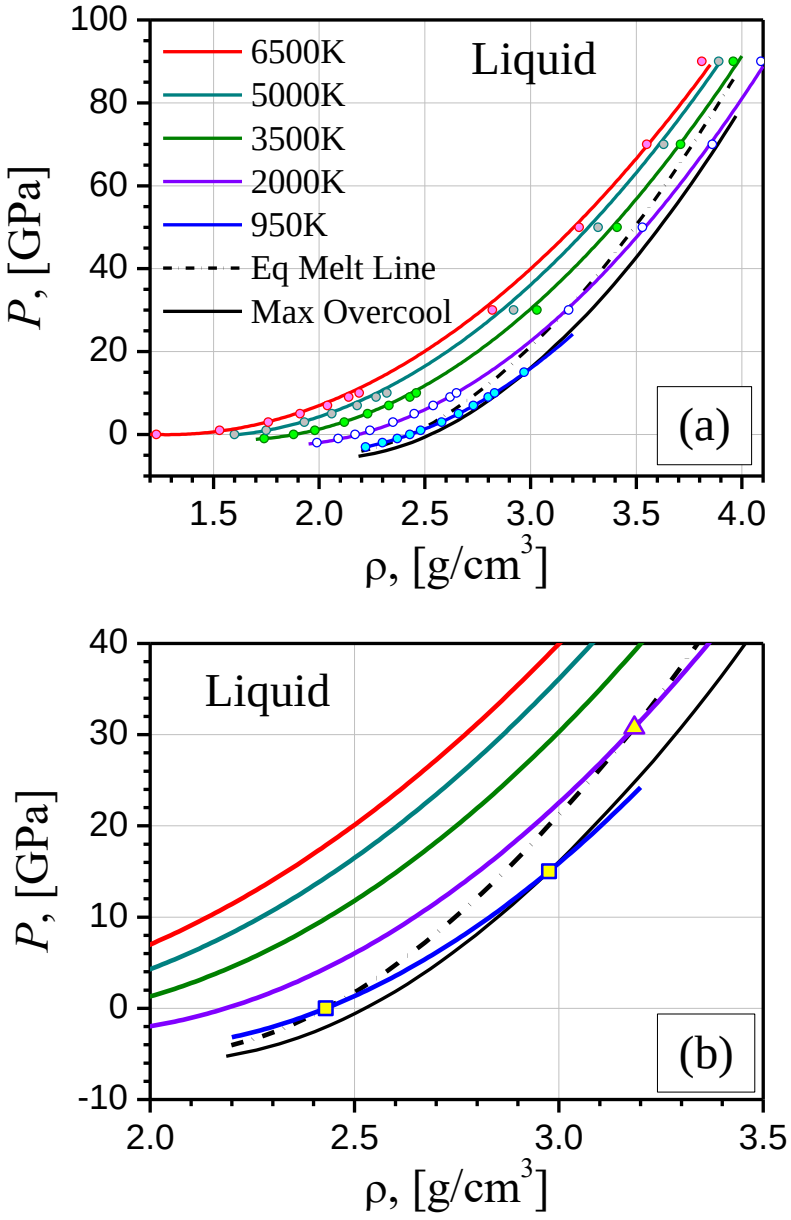

Fig.2. Isotherms for the liquid phase.

4.2 Caloric equation of state *E(ρ,T)*

The same initial configuration of 23328 atoms was used to determine the caloric equation of state. The sample was heated to a predetermined temperature and left in these conditions for 1 ns at a constant pressure set by the barostat. Density and internal energy were recorded as the sum of kinetic and potential interaction energies of all particles. The results of these measurements are given in Tables 3(a) and 4 (a) of the appendix.

Next, an approximating function similar to the previous paragraph was constructed:

$$\begin{aligned} \varepsilon(\rho,T) &= a(T)\rho^2 + b(T)\rho + c(T) \\ a(T) &= \alpha_a T^2 + \beta_a T + \gamma_a \\ b(T) &= \alpha_b T^2 + \beta_b T + \gamma_b \\ c(T) &= \alpha_c T^2 + \beta_c T + \gamma_c \end{aligned} \qquad (3)$$

Here the energy dimension is kJ/g. The values of the coefficients α, β, γ for the solid and liquid phases are given in table. 3(b) and 4(b) of the appendix.

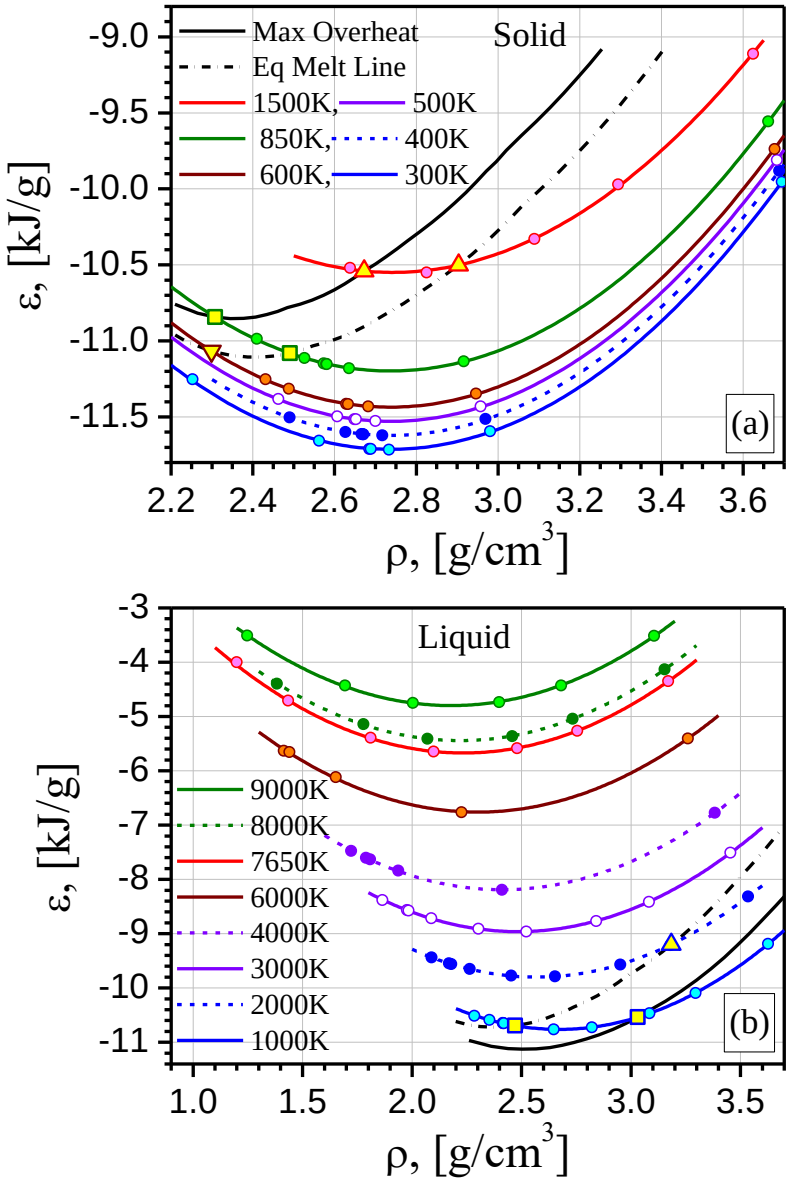

Fig.3. Energy isotherms for the solid (a) and liquid (b) phases.

The range of applicability of the approximating function for the solid phase corresponds to the extreme values of Table 3(a).

For the liquid phase, the obtained approximation is applicable only up to a critical temperature of 7650K. At higher temperatures, it is proposed to use a parabolic approximation in density (as before)

$$\varepsilon(\rho,T) = a(T)\rho^2 + b(T)\rho + c(T), \tag{4}$$

while for the parameters *a(T), b(T), c(T)* - linear interpolation between the values given in Table 4(b).

In Figure 3, the circles show the results of MD experiments for the solid (a) and liquid (b) phases, their approximation by the proposed method.

4.3 Thermodynamic consistency

In the theory of thermodynamic potentials, there is a well-known relation connecting the temperature derivative of pressure at constant density and the derivative of internal energy with respect to density at constant temperature:

$$\left(\frac{\partial P}{\partial T}\right)_\rho = \frac{1}{T}\left[P - \rho^2\left(\frac{\partial \varepsilon}{\partial \rho}\right)_T\right] \tag{5}$$

This relationship shows that thermal and caloric EOS cannot be arbitrary, but must be consistent with each other [25].

Using the approximating functions (2), (3) with the parameters of Tables 1(b), 3(b) for the solid phase, the left and right parts of the equation (5) were compared at zero pressure in the temperature range from 300 K to 1000 K. The result is shown in Figure 4(a). It can be seen that the degree of mismatch does not exceed 5% in this range.

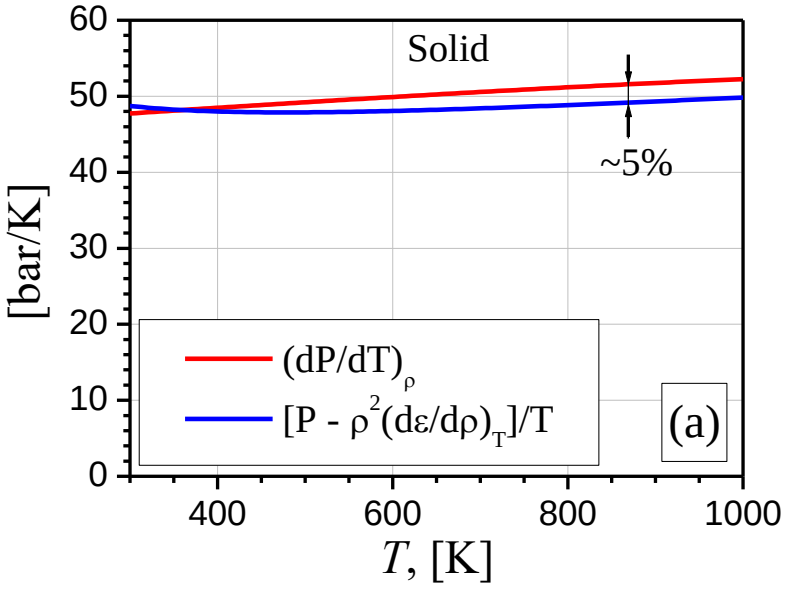

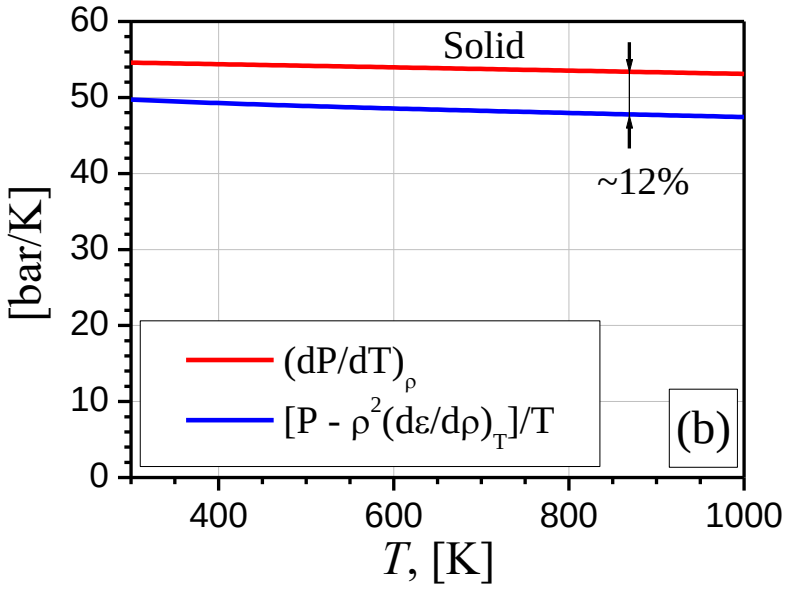

Fig.4. Consistency (solid phase) of the thermal and caloric EOS:
(a) calculated EOS, (b) EOS from Ref. [26]

The degree of thermodynamic consistency of the obtained equations of state (3), (4) was verified by comparison with the data of semi-empirical aluminum EOS given in the well-known work [26].

Having isolated the solid phase from these equations, we obtained a similar comparison of the left and right parts of the ratio (5) at zero pressure, shown in Fig. 4 (b). The degree of mismatch here was about 12%.

Thus, the degree of mismatch in our case is within acceptable limits.

5 CONCLUSIONS

1. Within the framework of a unified atomistic model, single-phase calorific and thermal equations of aluminum state in the temperature range from room to critical ($T_0 \le T < T_{cr}$) and pressure P ≤ 100 Gpa were obtained by the method of molecular dynamics.
2. Both equations of state are constructed in a smooth analytical representation form.
3. The thermodynamic consistency of the obtained equations is investigated, the mismatch of which does not exceed 5% in the region of applicability of the model.

Acknowledgements: The results were obtained using the equipment of Shared Resource Center of KIAM RAS (http://ckp.kiam.ru).

APPENDIX 1. THE RESULTS OF MEASURING IN MD EXPERIMENTS AND THE PARAMETERS OF APPROXIMATING FUNCTIONS OF THERMAL AND CALORIFIC URS FOR SOLID AND LIQUID PHASES OF THE MODEL AL

T=300K		T=600K		T=900K		T=1500K	
ρ, [g/cm^3]	P, [GPa]	ρ, [g/cm^3]	P, [GPa]	ρ, [g/cm^3]	P, [GPa]	ρ, [g/cm^3]	P, [GPa]
2.34	-7	2.28	-6	2.38	-3	2.63	5
2.41	-6	2.36	-5	2.46	-2	2.83	10
2.46	-5	2.43	-4	2.51	-1	3.09	20
2.52	-4	2.49	-3	2.56	0	3.29	30
2.56	-3	2.54	-2	2.61	1	3.47	40
2.61	-2	2.58	-1	2.69	3	3.62	50
2.65	-1	2.63	0	2.76	5	3.76	60
2.68	0	2.67	1	2.82	7	3.89	70
2.72	1	2.74	3	2.88	9	4.01	80
2.79	3	2.8	5	2.91	10	4.12	90
2.85	5	2.89	8	3.34	30		
2.9	7	2.95	10	3.66	50		
2.96	9	3.37	30	3.92	70		
2.98	10	3.68	50	4.15	90		
3.39	30	3.93	70				
3.69	50	4.16	90				
3.95	70						
4.17	90						

Table 1(a). Isotherms of the **solid** phase (results of MD modeling).

	$\alpha_{a,b,c}$	$\beta_{a,b,c}$	$\gamma_{a,b,c}$
a	-6.48059E-07	0.002105144	21.27285873
b	4.39592E-06	-0.014915725	-85.36042798
c	-7.01040E-06	0.029571398	74.42767645

Table 2(b). Coefficients of the analytical approximating function for the thermal EOS of the **solid** phase.

T=950K		**T=2000K**		**T=3500K**		**T=5000K**		**T=6500K**	
ρ, [g/cm^3]	P, [GPa]	ρ, [g/cm^3]	P, [GPa]	ρ, [g/cm^3]	P, [GPa]	ρ, [g/cm^3]	P, [GPa]	ρ, [g/cm^3]	P, [GPa]
2.22	-3	1.99	-2	1.74	-1	1.6	0	1.23	0
2.3	-2	2.09	-1	1.88	0	1.75	1	1.53	1
2.37	-1	2.17	0	1.98	1	1.93	3	1.76	3
2.43	0	2.24	1	2.12	3	2.06	5	1.91	5
2.48	1	2.35	3	2.23	5	2.18	7	2.04	7
2.58	3	2.45	5	2.33	7	2.27	9	2.14	9
2.66	5	2.54	7	2.43	9	2.32	10	2.19	10
2.73	7	2.62	9	2.46	10	2.92	30	2.82	30
2.8	9	2.65	10	3.03	30	3.32	50	3.23	50
2.83	10	3.18	30	3.41	50	3.63	70	3.55	70
2.97	15	3.53	50	3.71	70	3.89	90	3.81	90
		3.86	70	3.96	90				
		4.09	90						

Table 2(a). Isotherms of the **liquid** phase (results of MD modeling).

	$\alpha_{a,b,c}$	$\beta_{a,b,c}$	$\gamma_{a,b,c}$
a	-3.71767E-08	-0.000469412	18.11139074
b	-1.86369E-07	0.007393025	-74.66818769
c	4.58247E-07	-0.010379117	70.11789674

Table 2(b). Coefficients of the analytical approximating function for the thermal EOS of the **liquid** phase.

T=300K		**T=400K**		**T=500K**	
ρ, [g/cm^3]	ε, [kJ/g]	ρ, [g/cm^3]	ε, [kJ/g]	ρ, [g/cm^3]	ε, [kJ/g]
2.25271	-11.25298	2.49038	-11.50416	2.46239	-11.38212
2.56238	-11.65675	2.62665	-11.59959	2.60668	-11.49718
2.68478	-11.71060	2.66646	-11.61347	2.64834	-11.51484
2.68883	-11.71143	2.66951	-11.61430	2.65242	-11.51606
2.7331	-11.71543	2.67077	-11.61459	2.69995	-11.52712
2.98054	-11.59526	2.71677	-11.62196	2.95764	-11.4303
3.69429	-9.95371	2.96931	-11.51296	3.68235	-9.81008
		3.6884	-9.88166		
T=600K		**T=850K**		**T=1500K**	
ρ, [g/cm^3]	ε, [kJ/g]	ρ, [g/cm^3]	ε, [kJ/g]	ρ, [g/cm^3]	ε, [kJ/g]
2.43119	-11.25283	2.40965	-10.98655	2.63801	-10.52033
2.48823	-11.31526	2.52629	-11.11286	2.82512	-10.55027
2.62880	-11.41380	2.57333	-11.14800	3.08902	-10.32981
2.63308	-11.41564	2.57958	-11.15181	3.29427	-9.97038
2.68229	-11.43067	2.58120	-11.15291	3.62428	-9.11196
2.94604	-11.34705	2.63519	-11.18040		
3.67651	-9.73753	2.91623	-11.13519		
		3.66132	-9.55658		

Table 3(a). Energy isotherms of the **solid** phase (results of MD modeling).

	$\alpha_{a,b,c}$	$\beta_{a,b,c}$	$\gamma_{a,b,c}$
a	-8.35937E-08	9.63648E-05	1.898023321
b	4.33686E-07	-0.000500128	-10.39682318
c	-5.10344E-07	0.001525898	2.25649827

Table 3(b). Coefficients of the analytical approximating function for the caloric EOS of the **solid** phase.

T=1000K		**T=2000K**		**T=3000K**		**T=4000K**	
ρ, [g/cm^3]	ε, [kJ/g]	ρ, [g/cm^3]	ε, [kJ/g]	ρ, [g/cm^3]	ε, [kJ/g]	ρ, [g/cm^3]	ε, [kJ/g]
2.28487	-10.51107	2.08905	-9.4399	1.86544	-8.38343	1.72233	-7.47671
2.35338	-10.58922	2.16958	-9.54698	1.97738	-8.56645	1.79054	-7.60137
2.41415	-10.64688	2.17908	-9.55854	1.98455	-8.57714	1.80849	-7.633
2.41669	-10.64916	2.26323	-9.64814	2.08802	-8.71731	1.93763	-7.84065
2.41927	-10.65153	2.453	-9.77298	2.303	-8.90906	2.41093	-8.19419
2.48557	-10.70028	2.65307	-9.78517	2.522	-8.96058	3.38288	-6.77325
2.647	-10.76111	2.952	-9.56904	2.841	-8.76869		
2.82138	-10.72659	3.181	-9.21049	3.082	-8.41509		
3.085	-10.46745	3.53486	-8.31323	3.45441	-7.51078		
3.295	-10.09354						
3.626	-9.19						
T=6000K		**T=7650K**		**T=8000K**		**T=9000K**	
ρ, [g/cm^3]	ε, [kJ/g]	ρ, [g/cm^3]	ε, [kJ/g]	ρ, [g/cm^3]	ε, [kJ/g]	ρ, [g/cm^3]	ε, [kJ/g]
1.41476	-5.63329	1.2	-4	1.38318	-4.3946	1.24702	-3.50836
1.44015	-5.65684	1.43395	-4.70802	1.77815	-5.14191	1.69447	-4.43125
1.65226	-6.11903	1.81063	-5.39192	2.07129	-5.40899	2.00357	-4.75185
2.22577	-6.76324	2.09914	-5.64564	2.4576	-5.36425	2.39819	-4.73628
3.2597	-5.40577	2.47961	-5.58607	2.73446	-5.04331	2.68073	-4.42846
		2.755	-5.26193	3.15393	-4.13077	3.10573	-3.51387
		3.17035	-4.35009				

Table 4(a). Energy isotherms of the **liquid** phase (results of MD modeling).

	$\alpha_{a,b,c}$	$\beta_{a,b,c}$	$\gamma_{a,b,c}$
a	1.14344E-08	-0.000128084	1.823425536
b	-7.75745E-08	0.00101952	-10.03976977
c	1.02945E-07	-0.00080964	2.089811385

Table 4(b). Coefficients of the analytical approximating function for the caloric EOS of the **liquid** phase (upto the temperature of 7650K)

T,[K]	$a(T)$	$b(T)$	$c(T)$
7650	1.508325756	-6.741328093	1.860939682
8000	1.501941928	-6.668241278	1.958913328
9000	1.491764258	-6.50320304	2.289158456

Table 4(c). Coefficients of the approximating parabolas over density for the caloric EOS of **liquid** (above the temeprature of 7650K)

REFERENCES

[1]. A.V. Bushman, V.E. Fortov, "Model equations of state", *Sov. Phys. Usp.*, **26**(6), 465–496 (1983). Doi:10.1070/pu1983v026n06abeh004419.

[2]. A. Otero-de-la-Roza, D. Abbasi-Pérez, V. Luaña, "Gibbs2: A new version of the quasiharmonic model code. II. Models for solid-state thermodynamics, features and implementation", *Comp. Phys. Commun.*, **182**(10), 2232-2248 (2011). Doi:10.1016/j.cpc.2011.05.009

[3]. E.D. Chisolm, S.D. Crockett, D.C. Wallace, "Test of a theoretical equation of state for elemental solids and liquids", *Phys. Rev. B*, **68**(10), 104103 (2003). Doi:10.1103/PhysRevB.68.104103

[4]. S.V.G. Menon, B. Nayak, "An Equation of State for Metals at High Temperature and Pressure in Compressed and Expanded Volume Regions", *Condensed Matter*, **4**(3), 71 (2019). Doi:10.3390/condmat4030071

[5]. V.E. Fortov, I.V. Lomonosov, "Equations of State of Matter at High Energy Densities", *TOPPJ*, **3**, 122-130 (2010).

[6]. L.V. Al'tshuler, R.F. Trunin, V.D. Urlin, V.E. Fortov, A.I. Funtikov, "Development of dynamic high-pressure techniques in Russia", *Sov. Phys. Usp.*, **42**(3), 261-280 (1999). Doi:10.1070/PU1999v042n03ABEH000545

[7]. *Physics of High Energy Density*, P. Calderola, H. Knopfel, (Eds.), Academic, New York, (1971).

[8]. G.A. Mourou, T. Tajima, S.V. Bulanov, "Optics in the relativistic regime", *Rev. Mod. Phys.*, **78**(2), 309-371 (2006). Doi: 10.1103/RevModPhys.78.309

[9]. V.E. Fortov, "Intense shock waves and extreme states of matter", *Sov. Phys. Usp.*, **50**(4), 333–353 (2007). doi:10.1070/pu2007v050n04abeh006234

[10]. L.V. Al'tshuler, "Use of shock waves in high-pressure physics", *Sov. Phys. Usp.*, **8**(1), 52–91 (1965). Doi: 10.1070/PU1965v008n01ABEH003062

[11]. V.E. Fortov, "High Energy Densities in Laboratories", *Extreme States of Matter*, *Springer Series in Materials Science*, *Springer*, *Cham*., vol 216, 23–89 (2016). Doi:10.1007/978-3-319-18953-6_3

[12]. D.H.H. Hoffmann, V.E. Fortov, I.V. Lomonosov, V. Mintsev, N.A. Tahir, D. Varentsov, J. Wieser, "Unique capabilities of an intense heavy ion beam as a tool for equation-of-state studies", *Phys. Plasmas*, **9**(9), 3651–3654 (2002). Doi:10.1063/1.1498260

[13]. V.E. Fortov, "High-Power Lasers in High-Energy-Density Physics", *Springer Series in Materials Science*, 167–275 (2016). Doi:10.1007/978-3-319-18953-6_5

[14]. V.I. Mazhukin, M.M. Demin, A.V. Shapranov, A.V. Mazhukin, "Role of electron pressure in the problem of femtosecond laser action on metals", *Appl. Surf. Sci.*, **530**, 147227(1-9) (2020). Doi: 10.1016/j.apsusc.2020.147227

[15]. D.H.H. Hoffmann, A. Blazevic, P. Ni, O. Rosmej, M. Roth, N.A. Tahir, A. Tauschwitz, S. Udrea, D. Varentsov, K.Weyrich, Y. Maron, "Present and future perspectives for high energy density physics with intense heavy ion and laser beams", *Laser Part. Beams*, **23**(01), 47 – 53 (2005). Doi:10.1017/s026303460505010x

[16]. V.E. Fortov, D.H.H. Hoffmann, B.Y. Sharkov, "Intense ion beams for generating extreme states of matter", *Phys.-Usp.*, **51**(2), 109 (2008). doi:10.1070/pu2008v051n02abeh006420

[17]. Ch. Triola, "Model comparisons for two-temperature plasma equations of state", *Phys. Plasmas*, **29**(11), 112705 (2022). Doi: 10.1063/5.0110725

[18]. V. Zhakhovsky, Y. Kolobov, Ashitkov S. et al., "Shock-induced melting and crystallization in titanium irradiated by ultrashort laser pulse", *Phys. Fluids*, **35**(9), 096104 (2023). Doi:10.1063/5.0165622

[19]. A.L. Khomkin, A.S. Shumikhin, "Equation of state, composition, and conductivity of dense metal-vapor plasma", *High Temp.*, **52**(3), 328-336 (2014). Doi:10.1134/s0018151x14030158

[20]. L. Hallo, C. Mézel, A. Bourgeade, D. Hébert, E.G. Gamaly, S. Juodkazis, "Laser-Matter Interaction in Transparent Materials: Confined Micro-explosion and Jet Formation", T.J. Hall, S.V. Gaponenko, S.A. Paredes (Eds), *Extreme Photonics & Applications. NATO Science for Peace and Security Series B: Physics and Biophysics. Springer, Dordrecht*, 121–146 (2010). Doi:10.1007/978-90-481-3634-6_8

[21]. S.I. Anisimov, A.M. Prokhorov, V.E. Fortov, "Application of high-power lasers to study matter at ultrahigh pressures", *Sov. Phys. Usp.*, **27**, 181–205 (1984). Doi: 10.1070/PU1984v027n03ABEH004036

[22]. V.I. Mazhukin**,** A.A. Samarskii, "Mathematical Modeling in the Technology of Laser Treatments of Materials", *Surv. Math. Indus.*, **4**(2), 85-149 (1994).

[23]. N.A. Inogamov, V.A. Khokhlov, Y.V. Petrov, V.V. Zhakhovsky, "Hydrodynamic and molecular-dynamics modeling of laser ablation in liquid: from surface melting till bubble formation", *Opt. Quant. Electron*., **52**, 63 (2020). Doi:10.1007/s11082-019-2168-2

[24]. E.N. Avrorin, B.K. Vodolaga, V.A. Simonenko, V.E. Fortov, "Intense shock waves and extreme states of matter", *Phys.-Usp.*, **36**(5), 337–364 (1993). Doi:10.1070/pu1993v036n05abeh002158

[25]. L.D. Landau, E.M. Lifshitz, *Course of Theoretical Physics, Vol. 5: Statistical Physics, Part 1, Third Edition*, Oxford, Pergamon Press (1980).

[26]. I.V. Lomonosov, "Multi-phase equation of state for aluminum", *Las. Part. Beams*, **25**(04), 567-584 (2007). Doi:10.1017/s0263034607000687

[27]. I.V. Lomonosov, S.V. Fortova, "Review. Wide-range semiempirical equations of state of matter for numerical simulation on high-energy processes", *High Temp*., **55**(4), 585–610 (2017). Doi:10.1134/S0018151X17040113

[28]. F. Fetsch, T.E. Foster, N.J. Fisch, "Temperature separation under compression of moderately-coupled plasma", *arXiv:2303.11415 [physics.plasm-ph]*, 1-49 (2023). Doi:10.48550/arXiv.2303.11415

[29]. G.I. Kanel, V.E. Fortov, S.V. Razorenov, "Shock Waves and Extreme States of Matter", *Shock-Wave Phenomena and the Properties of Condensed Matter*, Springer, New York, NY, 301–319 (2004). doi:10.1007/978-1-4757-4282-4_8

[30]. V.E. Fortov, "Intense shock waves and extreme states of matter", *Phys.-Usp.*, **50**(4), 333–353 (2007). doi:10.1070/pu2007v050n04abeh006234

[31]. V.I. Mazhukin, "Kinetics and Dynamics of Phase Transformations in Metals Under Action of Ultra-Short High-Power Laser Pulses. Chapter 8", I. Peshko (Ed.), *Laser Pulses – Theory, Technology, and Applications*, 219 -276, InTech, Croatia (2012). Doi: 10.5772/50731.

[32]. E.G. Gamaly, A.V.Rode, "Review. Physics of ultra-short laser interaction with matter: From phonon excitation to ultimate transformations", Prog. Quant. Electron., **37**(5), 215-323 (2013). Doi:10.1016/j.pquantelec.2013.05.001

[33]. K.P. Migdal, D.K. Il'nitsky, Y.V. Petrov, N.A. Inogamov, "Equations of state, energy transport and two-temperature hydrodynamic simulations for femtosecond laser irradiated copper and gold", *J. Phys. Conf. Ser*., **653**, 012086 (2015). Doi:10.1088/1742-6596/653/1/012086

[34]. A. Ray, M.K. Srivastava, G. Kondayya, S.V.G. Menon, "Improved equation of state of metals in the liquid-vapor region", *Laser Part. Beams*, **24**(03), 437-445 (2006). doi:10.1017/s0263034606060381

[35]. C.J. Yocom, X. Zhang, Y. Liao, "Research and development status of laser peen forming: A review", *Opt. Las. Technol.*, **108**, 32–45 (2018). doi:10.1016/j.optlastec.2018.06.032
[36]. A.V. Mazhukin, V.I. Mazhukin, M.M. Demin, "Modeling of femtosecond laser ablation of Al film by laser pulses", *Appl. Surf. Sci.*, **257**, 5443–5446 (2011). doi:10.1016/j.apsusc.2010.11.154
[37]. V.I. Mazhukin, M.M. Demin, A.V. Shapranov, "High-speed laser ablation of metal with pico- and subpicosecond pulses", *Appl. Surf. Sci*., **302**, 6–10 (2014). Doi:10.1016/j.apsusc.2014.01.111
[38]. V.I. Mazhukin, M.M. Demin, A.V. Shapranov, I. Smurov. "The method of construction dynamically adapting grids for problems of unstable laminar combustion", *Numer. Heat Transf. B: Fundam.*, **44(**4), 387 – 415 (2003). Doi: 10.1080/10407780390219469
[39]. A.V. Mazhukin, V.I. Mazhukin, "Dynamic Adaptation for Parabolic Equations", *Comput. Math. Math. Phys.*, **47(**11), 1833 – 1855 (2007). Doi: 10.1134/S0965542507110097
[40]. O.N. Koroleva, V.I. Mazhukin, "Mathematical Simulation of Laser Induced Melting and Evaporation of Multilayer Materials", *Comput. Math. Math. Phys.*, **46**(5), 848 – 862 (2006). Doi: 10.1134/S0965542506050095
[41]. V.I. Mazhukin, M.M. Chuiko, "Solution of multi-interface Stefan problem by the method of dynamic adaptation", *J Comput Methods Appl Math*, **2**(3), 283-294 (2002). Doi:10.2478/cmam-2002-0017
[42]. V.I. Mazhukin, V.V. Nossov, I. Smurov, "Modeling of plasma-controlled surface evaporation and condensation of Al target under pulsed laser irradiation in the nanosecond regime", *Appl. Surf. Scie.*, **253**, 7686 – 7691 (2007). Doi:10.1016/j.apsusc.2007.02.039
[43]. P.V. Breslavsky, V.I. Mazhukin, "Dynamically Adapted Grids for Interacting Discontinuous Solutions", *Comput. Math. Math. Phys.*, **47**(4), 687 – 706 (2007). Doi: 10.1134/S0965542507040124
[44]. V.I. Mazhukin, A.V. Mazhukin, M.G. Lobok, "Comparison of Nano- and Femtosecond Laser Ablation of Aluminium", *Las. Phys.*, **19**(5), 1169 – 1178 (2009). Doi: 10.1134/S1054660X0905048X
[45]. V.V. Zhakhovskii, N.A. Inogamov, Yu.V. Petrov, S.I. Ashitkov, K. Nishihara, "Molecular dynamics simulation of femtosecond ablation and spallation with different interatomic potentials", *Appl. Surf. Sci.*, **255**, 9592–9596 (2009). Doi:10.1016/j.apsusc.2009.04.082
[46]. L. Verlet, "Computer "Experiments" on Classical Fluids. I. Thermodynamical Properties of Lennard-Jones Molecules", *Phys. Rev.*, **159**, 98-103 (1967).
[47]. S. Plimpton, "Fast Parallel Algorithms for Short-Range Molecular Dynamics", *J. Comp. Phys.*, **117**(1), 1–19 (1995). Doi:10.1006/jcph.1995.1039

Received July 18, 2023